Mobility Sub-System for the Exploration Technology Rover

Randel Lindemann*, Lisa Reid*, and Chris Voorhees*

Abstract

A new six-wheeled robotic roving vehicle was developed for NASA's Exploration Technology (ET) program. The rover which is called the Field, Integrated, Design, and Operations (FIDO) rover is being used for advanced technology development [1]. In addition, copies of FIDO's Mobility Sub-System (MSS) are being used for software development in several NASA projects, including the prototype for the flight Athena Rover of the Mars Sample Return (MSR) project's 2003 mission. The focus of this paper is the work done on the MSS, specifically the development and test of the wheel drive actuators, which are fundamental to vehicle mobility.

Introduction

The Exploration Technology Rover (ET Rover) project developed a vehicle for multi-kilometer desert field operations in anticipation of the next suite of Mars missions [2]. FIDO represents the next step in the evolution of planetary rovers after the Sojourner rover of the Mars Pathfinder mission [3]. The next generation rover is envisioned as a highly autonomous and long range mobile science and sample collection system. This paper describes the design, assembly, and test of the essential mechanical, structural, and mobility aspects of the FIDO rover contained in the MSS and shown in Figure 1.

FIDO is an independently servoed six-wheel drive, six-wheel steered vehicle. The MSS is the mechanical and structural hardware that is associated with the FIDO rovers frame, suspension, actuation and running gear. Specifically, the MSS is comprised of four major Assemblies; a left and right rocker-bogie suspension, a chassis or frame, and the solar-power structural assembly called the "Strongback". The rocker-bogie suspension is a scaled-up Mars Pathfinder Sojourner rover design [4]. The rocker-bogies connect to the main body or chassis of the rover via a geared internal differential through two structural members called the Jeff tubes. The chassis serves the same roles, except thermal isolation, for FIDO that the Warm Electronics Box (WEB) performed for the Sojourner rover [5]. Affixed to the top of the chassis is the Strongback, which is a stiff, strong and light-weight structure for the mounting of solar cells, as well as engineering and science payload items. Additional copies of the ET Rover MSS are also being fabricated for other technology development efforts. Software development for the Athena rover of the MSR 2003 flight project will be completed utilizing a MSS, and several R&D rovers at various NASA centers and Universities will be built around an MSS base.

* Jet Propulsion Laboratory-California Institute of Technology, 4800 Oak Grove Dr., Pasadena, CA

Project Goals and Requirements

The level 1 goal of the ET Rover project was to develop and field test a flight relevant rover for multi-kilometer science and sampling sorties in the Mojave Desert of California within 16 months of project conception. Also, a goal was accepted to facilitate other advance technology projects, as well as the MSR flight project by providing the initial rover MSS for their control algorithm and software development efforts. The delivery to the MSR flight project became the basis for the Software Development Model (SDM) rover. Design drivers were taken from flight and technology sources and a best fit was achieved that allowed FIDO to be baselined as the flight projects "breadboard", or prototype, rover.

The ET project's schedule constraints required that the mechanical system be designed, fabricated, and assembled within 8 months of project funding. The goal that the rover would be flight relevant, without a complete definition of the flight projects mission architecture was in keeping with NASA's faster, better, cheaper paradigm. Many assumptions about the directions that the flight rover design was or would be going were elevated to requirements for the MSS design effort.

The basic vehicle kinematics was taken as an extension of the Sojourner flight rover, which provided heritage by its mobile functionality on Mars. The Sojourner mechanical system was scaled up in size to increase the available payload capability for science and rock sampling, as well as to increase the vehicle's mobility in the hazardous environment of sandy, hilly, rock strewn fields [6]. The MSS was scaled in size to Sojourner by increasing the wheel diameter and similarly scaling all of the rocker-bogie suspension parameters. The rest of the requirements that were accepted from the Athena Rover include:

(1) The use of permanent-magnet brushed D.C. motors with integral quadrature encoding, based on Honeywell IR emitter-detector pairs, as well as integral and passive magnetic detent brakes [7].

(2) Thrust force capability from each wheel drive at motor stall equal to 1/2 the vehicles projected weight. The vehicle speed should be more then 6 cm/sec. Because of a lack of understanding of the torque and speed requirements for steering, the steering drive design is similar to that of the wheel drive.

(3) A scaled up Sojourner style rocker-bogie was utilized on all kinematic or geometric parameters of the rocker-bogie suspension. The chassis was sized to be identical in internal volume to an early conceptual flight Athena Rover WEB at the time of "requirements freeze" for the MSS.

(4) An additional sensing requirement was placed on the rocker-bogie suspension for utilizing flight like potentiometers in the steering drives, in addition to the quadrature

encoding detent devices, as well as in the bogies and the rocker arms of the suspension.

MSS Design

The MSS consists of four major assemblies: the left and right rocker-bogie suspensions, the chassis, and the Strongback. The MSS with two payload elements, a stowed mast and deployed instrument arm, attached to the Strongback is shown in Figure 2. The rover's wheelbase and track form a square footprint. The external cylindrical surface of each wheel is the 'tire' and is threaded for the fastening of cleats and spikes for traction in both soft and hard terrain.

The rocker-bogies provide a passive suspension with three degrees-of-freedom (dof). The first two dofs are the free rotation of each bogie about its pivot to the rocker arm. This rotation is measured by a potentiometer inside the pivot housing. The two rocker arms are connected on either side of the chassis to the Jeff tubes, which are used to connect the rocker arms to the internally geared differential inside the bottom of the chassis. Therefore, between the left and right rocker arms there is only a single dof, which is a rotation measured at the differential by a gear-reduced potentiometer. The full range rotation of the rocker arms is also limited by the use of a hardstop on the underside of the Strongback.

There are three wheel drive and steering assemblies on each rocker-bogie suspension assembly. The major features of the wheel drive gear train include the motor, gearing, and bearings. Figure 3 shows a cross section view of the wheel drive and steering assembly. The motors used are Maxon D.C. motors using Neodymium Iron Boron (NdFeB) magnets and graphite brushes. Attached to the motor is an integral single stage planetary gearhead.

The output shaft of the motor and planetary gearhead is connected to a spur gear pinion. The spur gear pinion is a pin hub style with 64 pitch. The spur gear pinion turns the hubless spur gear.

A drive shaft connects the output of the spur gear to the input of the harmonic drive by HD Systems. The input of the harmonic drive is a standard oldham coupling configuration to comply to small shaft misalignment. One of the oldham coupling pieces is modified to shorten its length and to expansion fit the drive shaft into it. There is also a clamping plate, which slip fits, by way of two alignment pins, to the flexspline. These pins provide an interface to the output of the harmonic drive. The drive shaft is supported inside the harmonic drive by the clamping plate and by the structure of the drive housing using small flanged ABEC-7 ball bearings.

The inner part of the wheel interfaces to the outside of the drive housing by two Kaydon Reali-Slim ball bearings. One of the bearings is a C-type (or radial contact) bearing with a seal on one side. The races and balls are lubricated with a general purpose grease.

The balls are coated with Endurakote, a special corrosion resistant coating provided by Kaydon, which together with the seal, protect the bearing from dirt and sand during rover operations. The second bearing is an X-type (or four-point contact) bearing. The races and balls are lubricated with a general purpose grease. There is no seal on this bearing as it is fully contained within the drive housing and wheel structures.

The wheel drive assembly is connected to the steering assembly with a wheel strut, as shown in Figure 3. The wheel strut is a bonded and riveted assembly of three square tubes. The top and bottom tubes are 90 deg bends and the middle section is a straight tube. The wheel strut assembly is in turn bonded and riveted to the wheel drive housing and steering hub of the steering assembly.

For lack of better clarity on torque and speed needs for the steering functions, the design of the steering actuators is similar to the wheel drives. The steering drives use the same Maxon motor gearhead combination and harmonic drive component set as used in the wheel drives. One major change in the steering gear train is the use of a 90 deg bevel gear set instead of the spur gears as used in the wheel drive gear train.

Another difference is that the steering assembly uses smaller Kaydon bearings to interface between the steering housing and steering hub. The bearings are A-type (or angular contact) bearings. The races and balls are lubricated with a general purpose grease. They are mounted as pairs in a back-to-back configuration. These bearings have no seals on them. To prevent contamination of the one exposed bearing, a spring energized Teflon seal, manufactured by Bal-Seal, was used in between the steering housing and steering hub. The seal is a housing-mounted flanged rotary seal. The seal is energized with an internal canted-coil spring. The seal material was chosen for its excellent wear resistance and low friction. The last significant design difference inbetween the steering assembly and the drive assembly is the use of a potentiometer. The precision potentiometer is made by BI Technologies.

Each motor in the wheel drive and steering assemblies includes a detent encoder device (DED). The DED uses magnet pairs as the passive detent brakes. The encoder consists of a GaAs IR emitting diode and a silicon phototransistor. In each DED assembly two emitter/detector pairs are used to provide quadrature.

Testing and Results

After assembly of the MSS, the mechanical team delivered the vehicle for integration with the electronics, sensors, and payload. Once the integration phase was completed the next step in the project was to begin software development and test. The extremely tight project schedule for the ET Rover task precluded highly desired mobility testing at the MSS stage of assembly and integration. Therefore, a series of tests was done on the fully integrated and functional FIDO vehicle in late January of 1999.

The plan centered on testing of the wheel drive actuators under various mobility-related loading conditions, and to test by default the overall vehicle's capability to perform in rough terrain. In addition, the tests were to determine that assembly and integration had been performed well, this is often called a "workmanship" test. The close similarity of the performance of each of the six wheel drives to one another under different conditions would determine an "acceptable" vs. a "not acceptable" condition. For comparison, a single spare wheel drive assembly was also tested on the bench top by directly driving the dc motor from a power supply.

The first test planned was to control all of the wheel drives on FIDO in a "freewheel", or unloaded, case. This was accomplished by placing the vehicle on a lab fixture that uses a shop jack to lift and move equipment. All of our tests used the current maximum setting on the vehicle speed. The second test involved driving FIDO on flat, horizontal, and hard ground. This test therefore radially loaded the wheel drives under the vehicle's own weight. The third test involved driving FIDO up a ramp incline, thus adding a significant tangential self-loading to the vehicle. This test was performed on a high friction surface: a PVC tarp on a wooden ramp. The fourth test was an obstacle-climbing test performed on a large plywood base, which was placed horizontal to the ground. The plywood base had an attached obstacle, or "wall", of one wheel diameter in height. The wall was made by nailing wood "2 by 4's" one on top of another to the center of the plywood base, spanning from side to side. The plywood and "2 by 4's" resembled a high friction surface with a centered vertical bump, so that the vehicle had to climb the obstacle simultaneously first with the front wheels, followed by the middle wheels, and finally the back wheels. The fifth and final test was to determine the vehicles floatation and mobility in dry, sifted desert sand, by having the vehicle attempt to climb a sand dune at the sand's angle of repose.

After full vehicle integration was completed it was found that the original system definition was not achieved by the electronics. The batteries were implemented at less than peak capacity and after all of the voltage drops through sub-system electronics were looked at, the peak voltage actually seen at the motors was found to be less. The result of this was to simply scale down the resulting performance expectation by the appropriate number of ratios. For instance, expected torque out of the motors would be scaled the ratio and mechanical power out of the motors would be scaled by the ratio squared.

The result of the freewheel test is shown in Figure 4, where the top graph indicates the current drawn by a representative wheel drive motor as a function of time, and the bottom graph indicates the wheel tangential speed. Because of the software control system developed for the rover, the commanded performance for all of the tests was a ramp up to a velocity profile for the cruise setting, followed by a ramp down velocity profile. The second test result shown in Figure 5 shows the performance of one of the wheels while the rover is driving on flat ground. The result for the third test is shown in Figure 6, where the rover was driven up a ramp, again commanded to ramp up to the specific velocity. The fourth test result shown for a single motor in Figure 7, shows the

performance of one wheel of the rover as the vehicle traverses a bump obstacle, or wall, completely spanning across its path. The fifth test shown in Figure 8, shows the current and speed as functions of time for the rover attempting to climb a sand dune, sifted to the angle of repose of the soil.

After all of the vehicle tests were performed, the data collected was analyzed. Figure 9 was generated to show the wheel drive actuators approximate performance in terms of the interrelationships between torque, speed, and current. The motor torque-speed-curve and current-speed relationships were given by the manufacturer. These specs were then scaled by the decrease in effective voltage at the motor windings. The three stages of gear reduction-were taken into account and directly scaled down the output speed of the actuator. The same gear reductions times their approximate spec efficiencies were then used to scale up the final output torque. The scaled line for the current axis is shown under the axis for torque, since torque is proportional to the current.

The graph in Figure 9 highlights key points taken from the wheel drive tests. From Figure 4, the average value of the of the no-load actuator current is found, which represents a value of motor torque reflected through the gearing stages, but fully lost after the output stage. The average current drawn during the level ground driving tests was found in Figure 5 and used to obtain an output torque average at each of the 6 wheels. The rated maximum continuous-power point, as reflected through the gear stages per the motor spec, is shown in Figure 9. By the time the torque demands are up to the maximum continuous rated capability, the actuator is no longer capable of maintaining the vehicle set point velocity. The required current draw for FIDO driving up an incline are found in Figure 6, with an output torque required shown in Figure 9. In Figure 7 the highest values of current drawn and output torque utilized are found for climbing the vertical wall of one wheel diameter in height. Two values are shown, an average peak magnitude and a maximum peak. The maximum peak values come very close to reaching the stalled motor condition. In Figure 8, the demands of driving up a sand dune at the angle of repose of the soil, approximately, is found to vary among the wheels due to slip at each of the wheels to the sand and the different level of loading on each wheel. The most highly loaded wheels, which are in the rear of the vehicle, pull up to a current level for an output torque required as shown in Figure 9.

Additional information about the ET Rover project, the FIDO rover and its development, as well as science related field trials can be found at the project's Web site given in Reference [8].

Conclusions

Overall, the FIDO rover and its MSS components performed as required and met the project goals for vehicle mobility. This was true, even with the impact to actuator capability of a less than advertised power sub-system range. The intrinsic margins utilized in the design process saved the day.

The project need to build a mechanical system in extremely short order to support the primary technology thrust of software and control system development places many demands on the mechanical design team. Decisions about the project's nominal requirements must be extrapolated from very high-level task descriptions and mission architecture, and many predictions must then be frozen into the requirements set. The very short schedule also diminishes the amount and depth of analyses that can be performed during the design stage, essentially limited to the so-called 'back of the envelope' type. Because of the typically much smaller budget than for a flight project, there is a reduction in the amount of resources that can be expended on fabrication services and procurements. The combined result is a very conservative and non-optimal design, based to a great extent on a combination of hardware heritage, cooperate knowledge, and best intuitions of the design team.

One difficulty encountered by the mechanical team during the testing phase was the inability to remove the software-control-electronics implementation out of the analysis of the results. The immaturity of the control software at the time of testing also made understanding the data very difficult. The testing results should best be seen as a qualification rather than quantification of the vehicle's capability.

The wheel drive actuators performed essentially as the design process predicted, but with a much larger range in the current and torque values seen at each drive than expected. The result was that no definitive workmanship "stamp of approval" could come from the simple no-load tests. The power draw and combined losses in the wheel drive actuators was larger than expected, but well within the given margins for the design.

The most demanding tests on the wheel drives and the vehicle are represented in the obstacle test and the sand dune test. The ability of the vehicle to traverse any obstacle in height up to the diameter of a wheel impressively met all of the rough terrain requirements. The vehicle's performance on the sand dune qualified its loose or low density terrain requirements. While the effective wheel slip for the case of FIDO traversing up a sand dune was measured to be in excess of 99%, the vehicle's flotation was not an issue. FIDO's ground pressure was too high for the rover to be an efficient dune crawler, but the vehicle could ultimately perform the traverse even though this was not a goal or requirement. An effective means to traverse areas of dunes with this class of vehicle simply requires that navigation take the rover around rather than straight up such a hill.

Acknowledgements

This work was performed at the California Institute of Technology's Jet Propulsion Laboratory, under contract with the National Aeronautics and Space Administration.

Reference herein to any specific commercial product, process or service by trade name, trademark, manufacturer, or otherwise does not constitute or imply its endorsement by the United States Government or the Jet Propulsion Laboratory.

References

1. Schenker, P. S., et al. "New Planetray Rovers for Long Range Mars Science and Sample Return." *Intelligent Robots and Computer Vision XVII: Algorithms, Techniques, and Active Vision SPIE Proceedings*, Vol. 3352, (November 1998), pp. 2-15.
2. Arvidson, R., et al. "FIDO: Field-Test Rover for 2003 and 2005 Mars Sample Return Missions." *Lunar and Planetary Society Conference*, (to be presented in 1999).
3. Matijevic, J. R., et al. "The Pathfinder Microrover." *Journal of Geophysical Research*, Vol. 102, No. E2, (25 February 1997), pp. 3989-4001.
4. Wilcox, B., A. Nasif and R. Welch. "Implications of Martian Rock Distributions on Rover Scaling." *International Conference and Mobile Planetary Robotics*, (January 1997).
5. Hickey, G. S., et al. "Integrated Lightweight Structure and Thermal Insulation for Mars Rover." *25th SAE International Conference on Enviromental Systems*, (July 1995).
6. Lindemann, R. A. "Quasi-Static Mobility Analysis Tool for the Design of Lunar/Martian Rovers and Construction Vehicles." *SAE International Off-Highway & Powerplant Congress and Exposition*, (September 1990).
7. Braun, D. and D. Noon. "Long Life DC Brush Motor for the Use on the Mars Surveyor Program." *32nd Aerospace Mechanisms Symposium*, (May 1998).
8. Baumgartner, E. "Exploration Technology Rover." http://robotics.jpl.nasa.gov/tasks/etrover/homepage.html (26 May 1998).

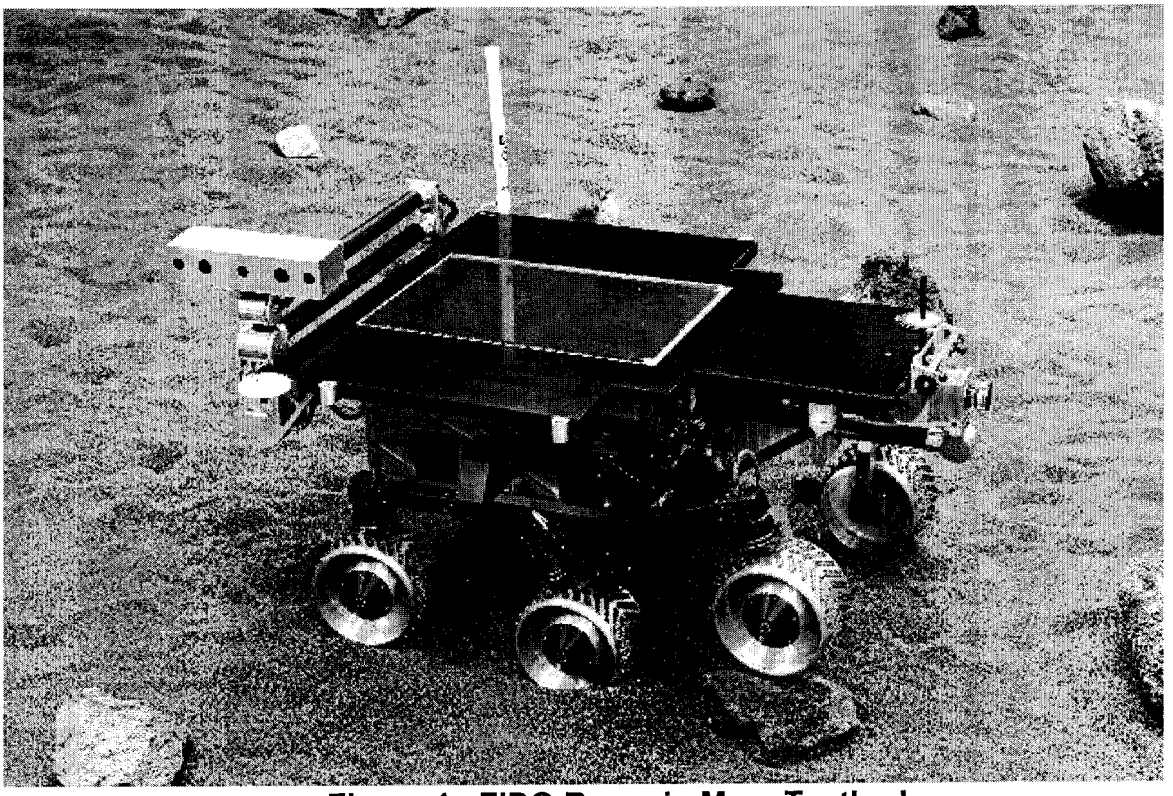

Figure 1. FIDO Rover in Mars Testbed

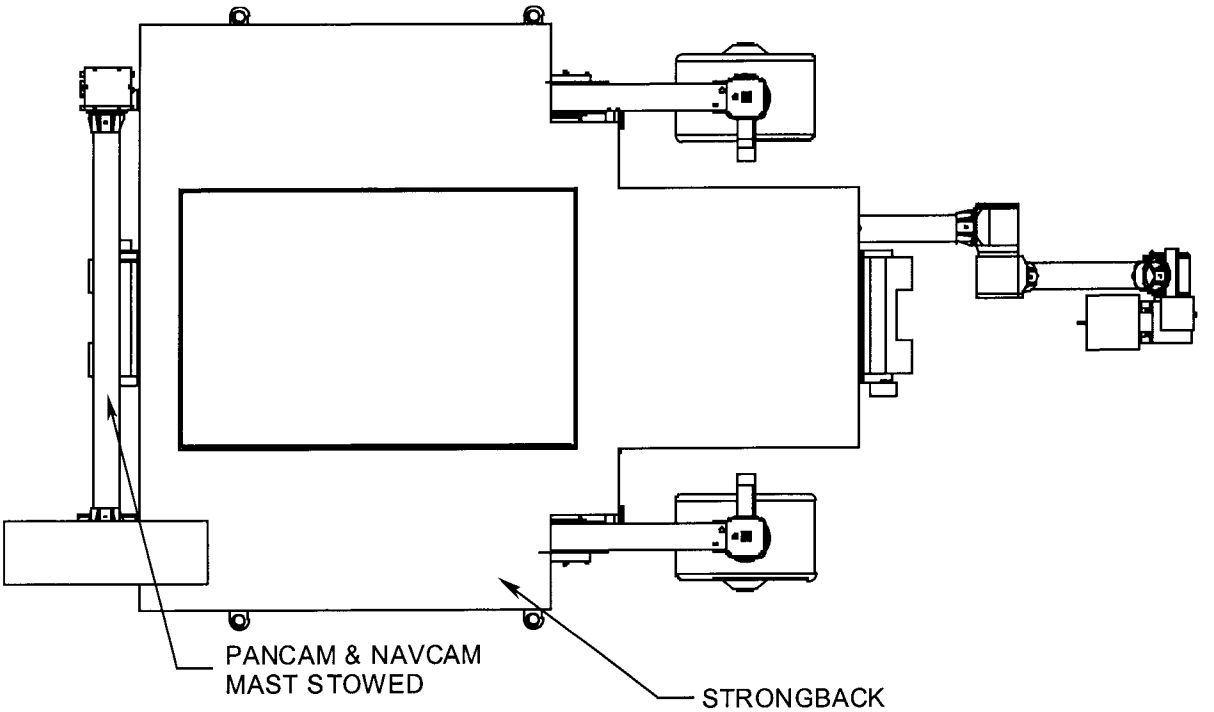
PANCAM & NAVCAM
MAST STOWED
STRONGBACK

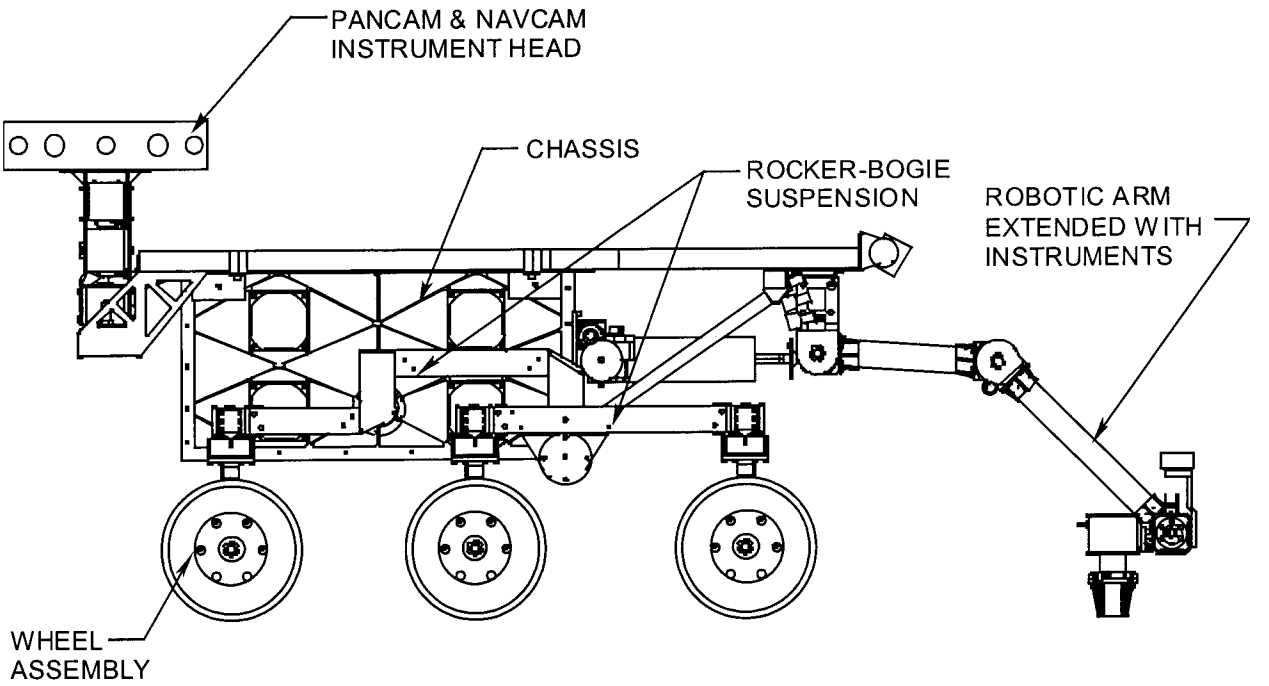
PANCAM & NAVCAM
INSTRUMENT HEAD
CHASSIS
ROCKER-BOGIE
SUSPENSION
ROBOTIC ARM
EXTENDED WITH
INSTRUMENTS
WHEEL
ASSEMBLY

Figure 2. FIDO Rover with Mast Stowed and Instrument Arm Deployed

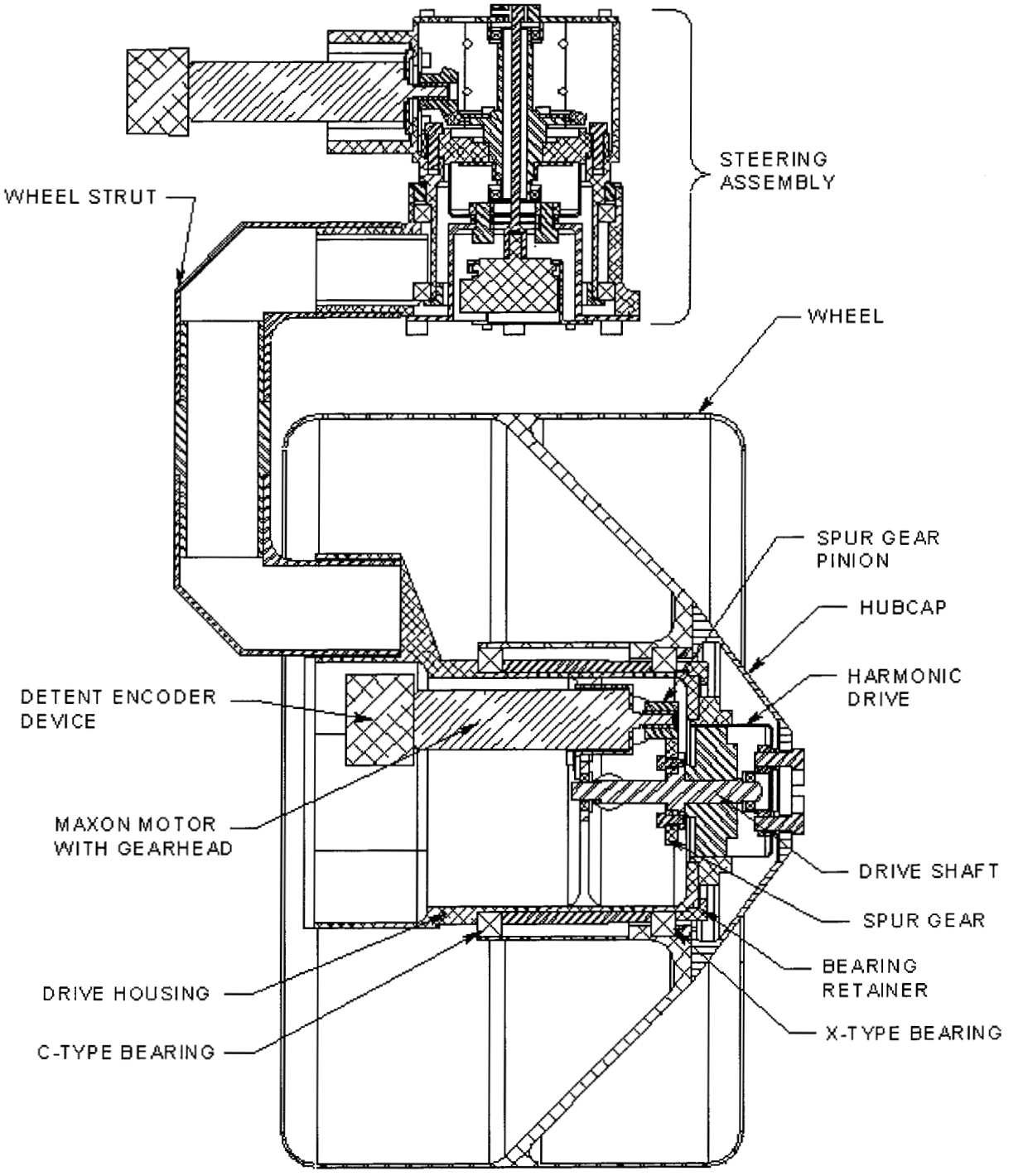

Figure 3. Wheel Drive and Steering Assembly

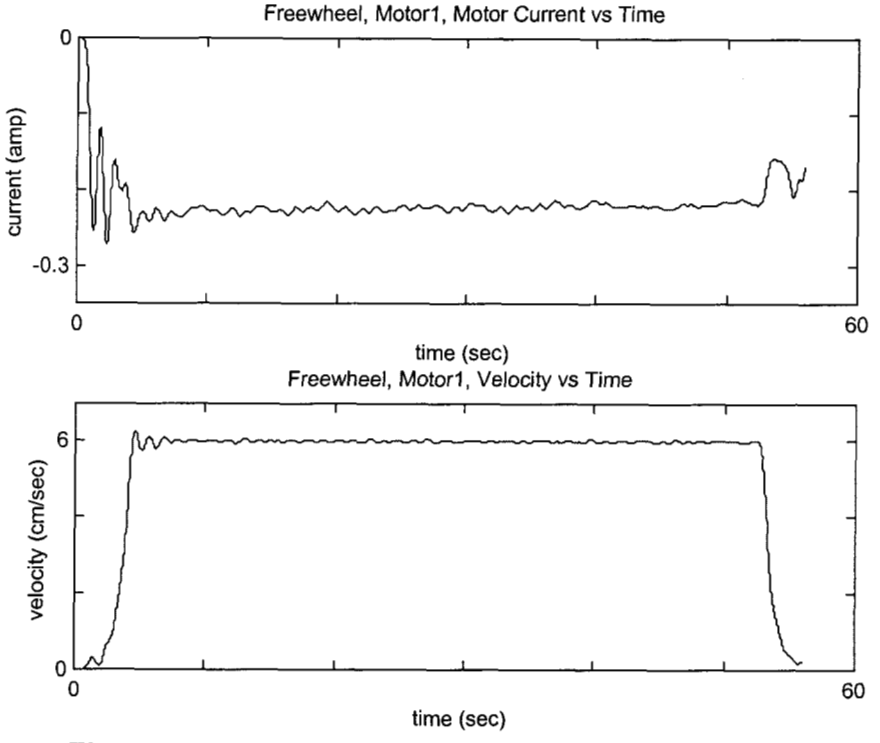

Figure 4. Freewheel Motor Current and Velocity

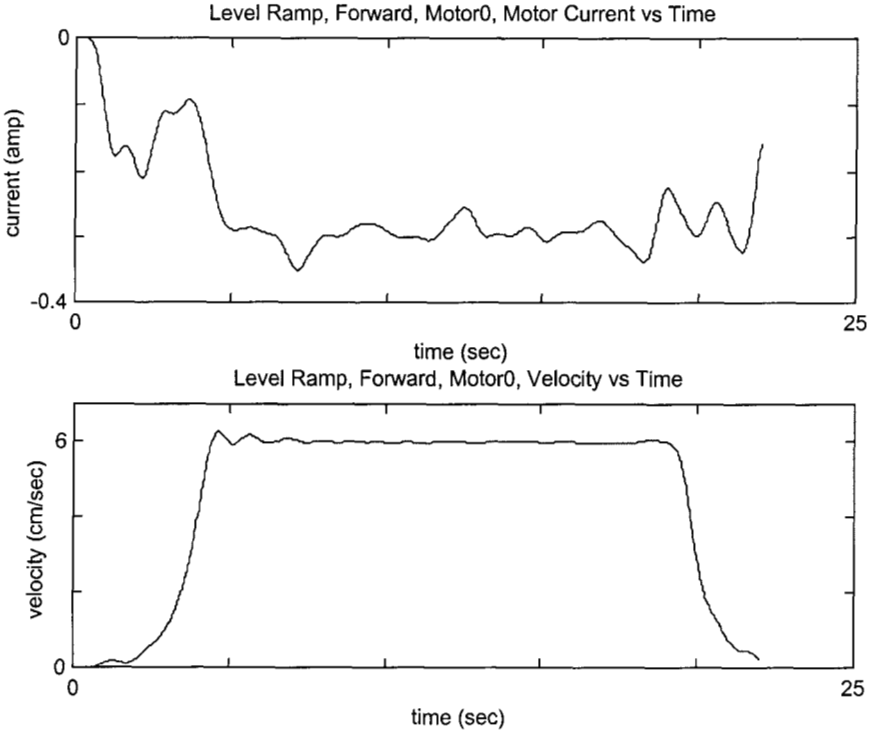

Figure 5. Forward on Level Ramp Motor Current and Velocity

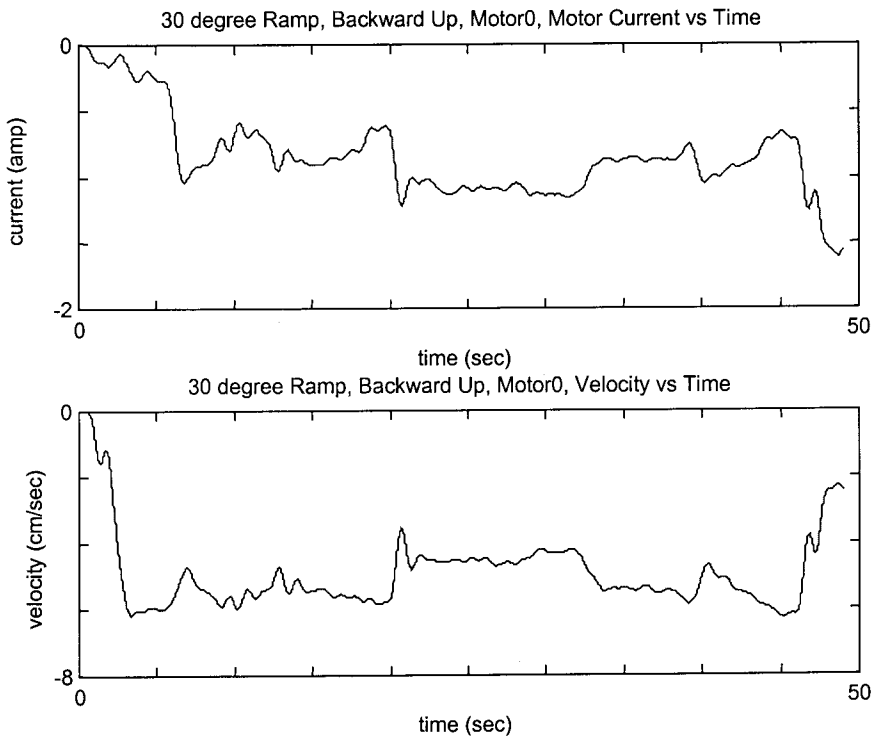

Figure 6. Backwards Up a 30 Degree Ramp Motor Current and Velocity

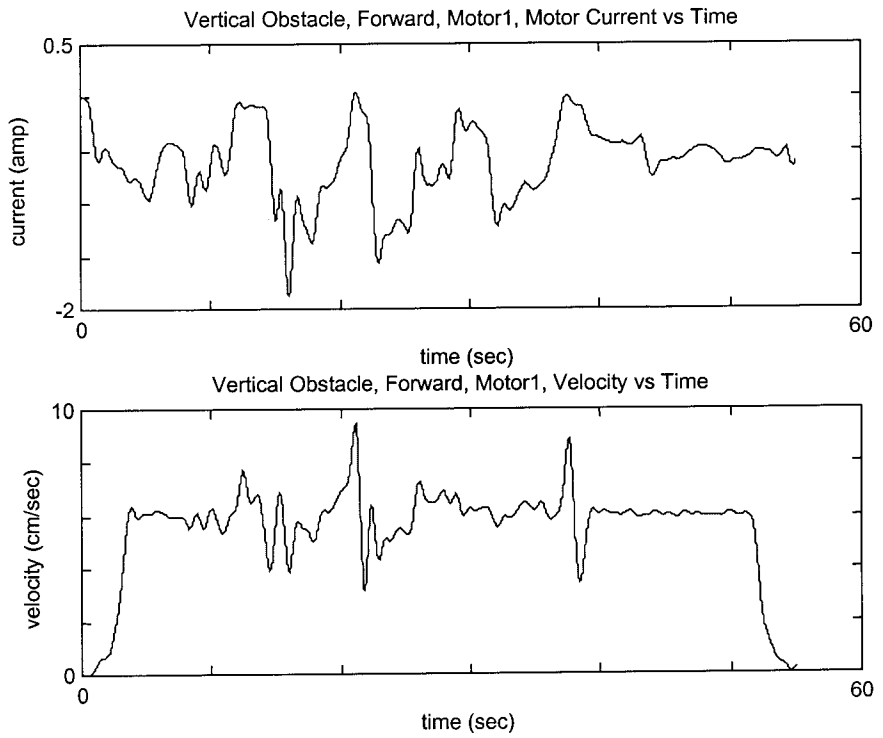

Figure 7. Forward Over Vertical Obstacle Motor Current and Velocity

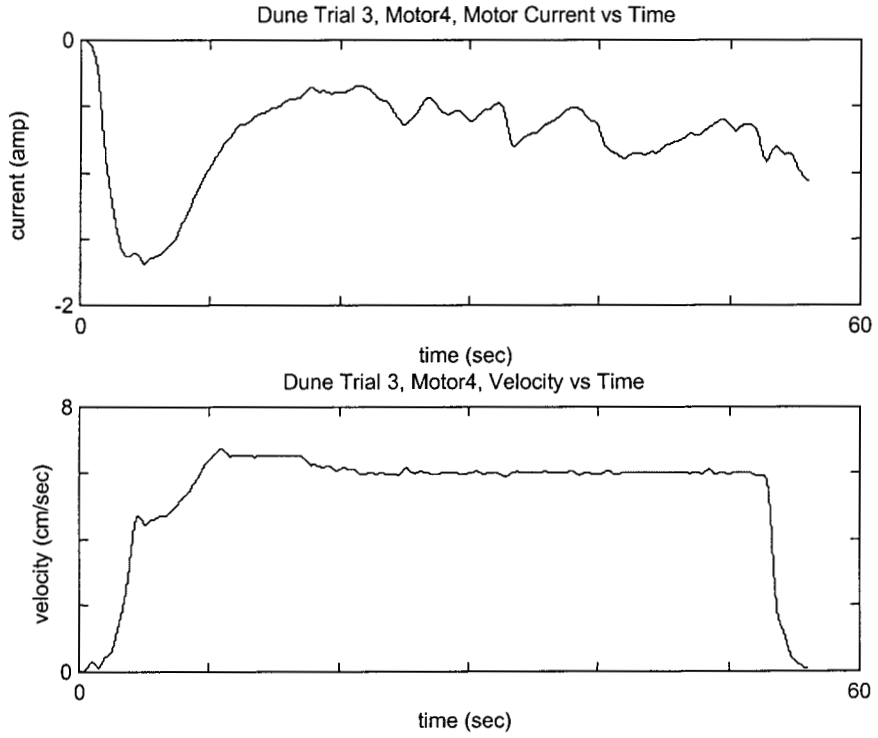

Figure 8. Dune Trial 3 Motor Current and Velocity

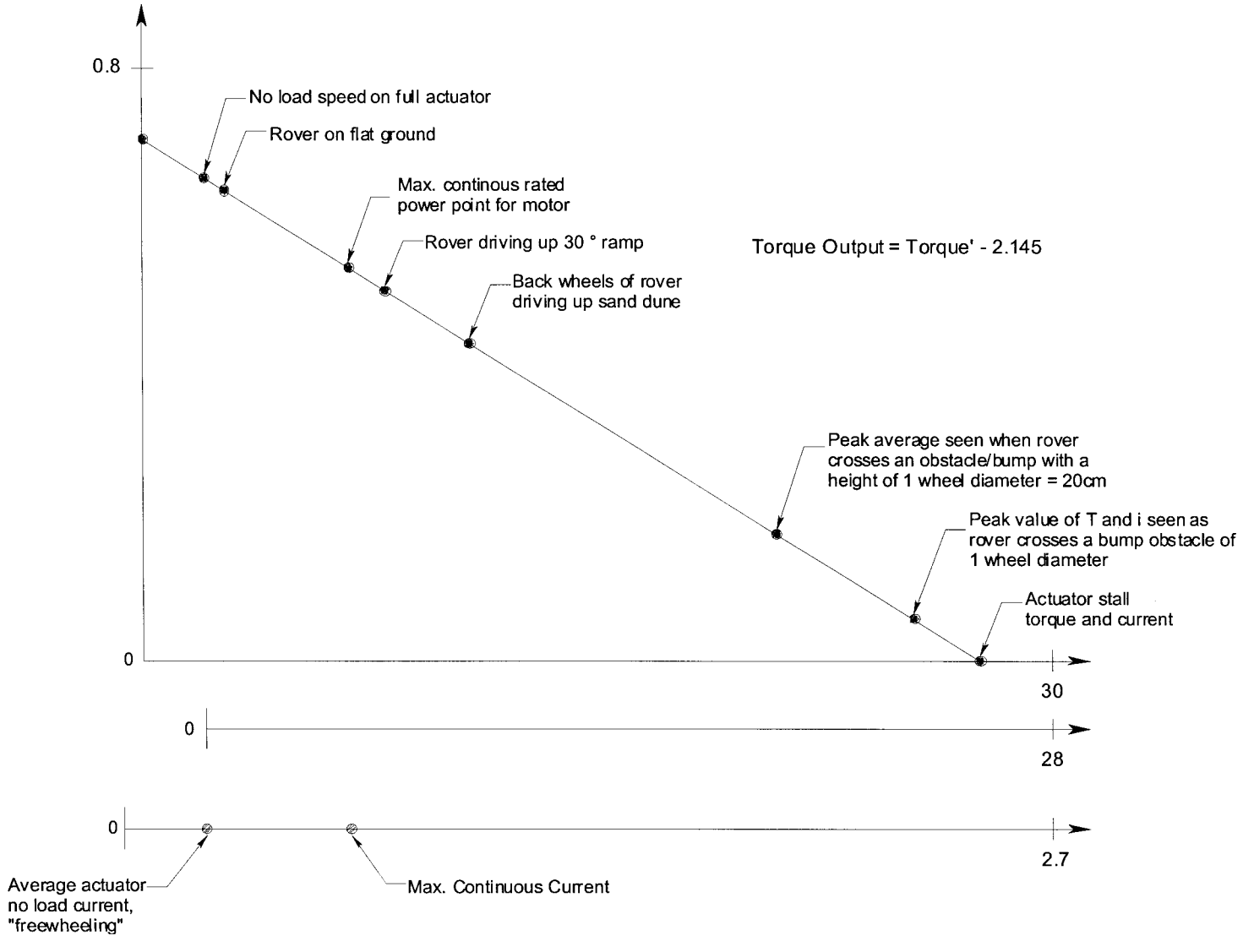
0.8
No load speed on full actuator
Rover on flat ground
Max. continous rated
power point for motor
Rover driving up 30 ° ramp
Back wheels of rover
driving up sand dune
Torque Output = Torque' - 2.145
Peak average seen when rover
crosses an obstacle/bump with a
height of 1 wheel diameter = 20cm
Peak value of T and i seen as
rover crosses a bump obstacle of
1 wheel diameter
Actuator stall
torque and current
0
30
0
28
0
2.7
Average actuator
no load current,
"freewheeling"
Max. Continuous Current
ω (rad/s)

$$f(T): \omega_{act} = -0.02507T + 0.724$$
$$f(i): \omega_{act} = -0.2.944i + 0.735$$

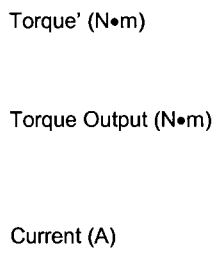

Figure 9. Actuator Torque-Speed-Current Relationships